

# Comparative study of the degradation of real textile effluents by photocatalytic reactions involving UV/TiO<sub>2</sub>/H<sub>2</sub>O<sub>2</sub> and UV/Fe<sup>2+</sup>/H<sub>2</sub>O<sub>2</sub> systems

J.C. Garcia, J.L. Oliveira, A.E.C. Silva, C.C. Oliveira,  
J. Nozaki<sup>†</sup>, N.E. de Souza<sup>\*</sup>

*Departamento de Química, Universidade Estadual de Maringá, Av. Colombo 5790, CEP 87020-900, Maringá, PR, Brazil*

Received 2 August 2006; received in revised form 24 November 2006; accepted 21 December 2006

Available online 30 December 2006

## Abstract

This work investigated the treatability of real textile effluents using several systems involving advanced oxidation processes (AOPs) such as UV/H<sub>2</sub>O<sub>2</sub>, UV/TiO<sub>2</sub>, UV/TiO<sub>2</sub>/H<sub>2</sub>O<sub>2</sub>, and UV/Fe<sup>2+</sup>/H<sub>2</sub>O<sub>2</sub>. The efficiency of each technique was evaluated according to the reduction levels observed in the UV absorbance of the effluents, COD, and organic nitrogen reduction, as well as mineralization as indicated by the formation of ammonium, nitrate, and sulfate ions. The results indicate the association of TiO<sub>2</sub> and H<sub>2</sub>O<sub>2</sub> as the most efficient treatment for removing organic pollutants from textile effluents. In spite of their efficiency, Fenton reactions based treatment proved to be slower and exhibited more complicated kinetics than the ones using TiO<sub>2</sub>, which are pseudo-first-order reactions. Decolorization was fast and effective in all the experiments despite the fact that only H<sub>2</sub>O<sub>2</sub> was used.

© 2007 Elsevier B.V. All rights reserved.

**Keywords:** Textile effluents; Titanium dioxide; Fenton reactions; Photodegradation; Mineralization

## 1. Introduction

The color of a water sample is related to the decrease in light intensity as it passes through the sample, mainly due to the presence of organic and inorganic material in the colloidal form. Industrial effluents such as textile industry ones are characterized by the gradual coloring of natural waters. Besides the negative effects on water appearance, which makes it repulsive to consumers, the presence of organic matter in the natural waters is directly associated with toxicity and carcinogenicity caused by dyes, surfactants, suspended solids, organochlorinated compounds, etc. that can be present in the effluent [1].

From an environmental point of view, decolorizing the washing bath is one of the greatest problems of the textile industry. It is estimated that more than 15% of the world dye production is released into the environment during synthesis, processing, and use. This is alarming since it means ca. 400 tonnes a day. This

loss is due mainly to incomplete dye fixing (10–20%) during the textile fiber dyeing step (Fig. 1) [2].

Several techniques such as membrane filtration, adsorption [3], coagulation [4], and biodegradation [5] have been used to solve the problems caused by the toxic substances contained in industrial effluents. However, all of these treatments result in secondary pollution, since they transfer the toxic substances from the liquid phase to other phases such as the sludge, used membranes, and saturated adsorbents, which cause another environmental problem. Therefore, there has been an increased interest in advanced oxidation processes (AOPs) that is an alternative destructive treatment in which chemical species are reduced into smaller fragments and even to the point of mineralization. AOPs are processes involving UV or visible radiation associated with substances such as H<sub>2</sub>O<sub>2</sub> [6], semiconductors such as TiO<sub>2</sub> [7], and ZnO [8], Fe<sup>2+</sup> or Fe<sup>3+</sup> [9], O<sub>3</sub> [10], and/or their variations and associations.

In this way, the aim of the present work is to compare the degradation behavior of real textile effluents using the following oxidation processes: UV/H<sub>2</sub>O<sub>2</sub>, UV/TiO<sub>2</sub>, UV/TiO<sub>2</sub>/H<sub>2</sub>O<sub>2</sub>, and UV/Fe<sup>2+</sup>/H<sub>2</sub>O<sub>2</sub>.

<sup>\*</sup> Corresponding author. Fax: +55 44 32614125.

E-mail address: [nesouza@uem.br](mailto:nesouza@uem.br) (N.E. de Souza).

<sup>†</sup> In memoriam.

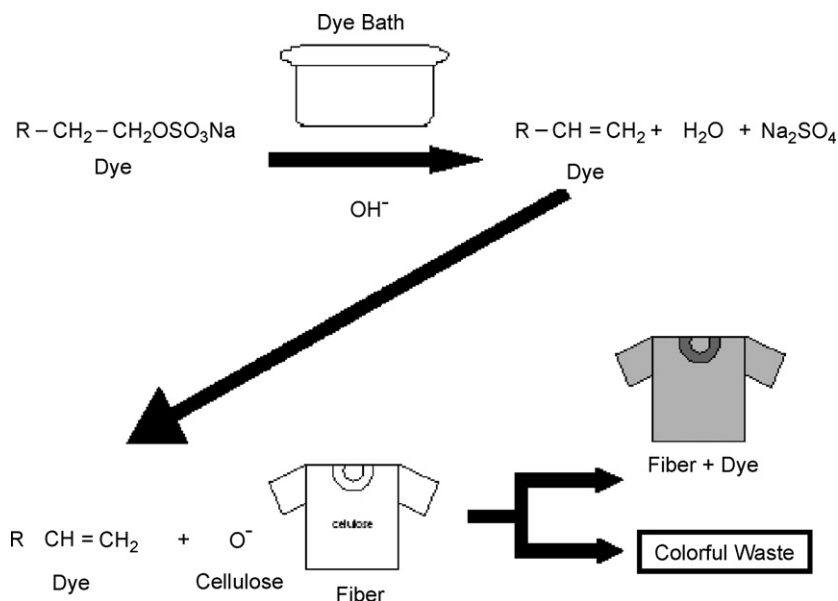


Fig. 1. Example of cotton dyeing with reactive dye.

## 2. Experimental procedures

### 2.1. Materials

The textile effluent samples (EFA, EFB, and EFC) presenting colorants (Yellow Procion, Red Procion, and Remazol Brilliant Blue R), sodium chloride, and surfactant agents as main the composition were kindly provided by a fabric manufacturer from the northwest region of Paraná State (PR), Brazil.  $\text{TiO}_2$  (P-25, 80% anatase, 20% rutile with a specific surface of  $50 \text{ m}^2 \text{ g}^{-1}$ ) was kindly provided by Degussa and used without previous purification.  $\text{H}_2\text{O}_2$  (30%, analytical grade) was purchased from Synth. All the other reagents were of the analytical grade and used without previous purification.

### 2.2. Photodegradation process

Irradiation was performed at ambient conditions in three open conic borosilicate glass reactors containing  $\text{TiO}_2$ ,  $\text{H}_2\text{O}_2$ ,  $\text{Fe}^{2+}$  or their associations at  $0.25 \text{ g L}^{-1}$ ,  $1 \times 10^{-2} \text{ mol L}^{-1}$ , and  $10.0 \text{ mg L}^{-1}$ , respectively. The samples were 500.0 mL of textile effluents collected on three different days (March, 2005) from the outlet of the dyeing machines, which have the pH adjusted previously by the industry from 13.0 to approximately 7.5 by using hydrochloride acid due to effluent waste reasons. The effluent samples were not diluted before the oxidation processes to avoid changes in their characteristics (Table 1).

### 2.3. Heterogeneous photocatalysis

UV/ $\text{TiO}_2$  system suspensions were sonicated for 20 min in the dark at pH 3.50, which was adjusted by addition of HCl  $0.10 \text{ mol L}^{-1}$  in order to reach the best adsorption rates that were attained in acid pHs (values determined in previous tests). The same procedure was performed for UV/ $\text{TiO}_2$ / $\text{H}_2\text{O}_2$  treatment with the addition of hydrogen peroxide after the sonication process.

### 2.4. Homogeneous photocatalysis

In the UV/ $\text{H}_2\text{O}_2$  and UV/ $\text{Fe}^{2+}$ / $\text{H}_2\text{O}_2$  treatments, pH was adjusted to 3.0 before addition of reagent of  $\text{Fe}^{2+}$  and  $\text{H}_2\text{O}_2$  reagents or their associations.

### 2.5. Photochemical reactor

The reagents plus the samples were continuously magnetically stirred in the photochemical reactor, with the surface of the solutions or suspensions approximately 30 cm distant from the radiation sources (three high pressure 250 W mercury lamps without bulb). The lamps were vertically fixed onto the top wall of a wooden box ( $80 \text{ cm} \times 80 \text{ cm} \times 50 \text{ cm}$ ). Four fans were placed in different positions on the side walls of the reactor to minimize the heating effect produced by the lamps. The internal walls were covered with aluminum foil to avoid radiation

Table 1  
Characteristics of the EFA, EFB, and EFC textile effluents samples

Effluents	pH	$\text{NH}_4^+$ ( $\text{mg L}^{-1}$ )	$\text{SO}_4^{2-}$ ( $\text{mg L}^{-1}$ )	$\text{N}_{\text{org}}$ ( $\text{mg L}^{-1}$ )	COD ( $\text{mg O}_2 \text{ L}^{-1}$ )
EFA	7.67	4.76	n.d.	12.00	808.12
EFB	7.39	4.48	n.d.	12.12	708.24
EFC	7.89	5.46	n.d.	12.14	799.04

n.d.: concentrations not detected due to effluent high coloring.

losses and the internal temperature ranged around 35 °C during irradiation process.

### 2.6. Analytical determinations

The degradation of the effluents as a function of irradiation time was monitored in quartz cuvettes (5 mL and 1 cm optical path) by using UV/vis spectrophotometry (Shimadzu 1240) at the wavelengths associated with simple aromatic (254 and 284 nm); conjugated aromatic (310 nm) and colored (430 nm) compounds. The mineralization rates were calculated by the Chemical Oxygen Demand (COD) decrease and by the oxidation of nitrogen and sulfur organic compounds to ammonium, nitrate, and sulfate ions. The used analytical techniques followed standard methods [11] and residual peroxide was determined according to the technique described by [12].

### 3. Results and discussion

Because of the evidences indicating that the degradation of organic substrates occurs on the surface of the catalyst, adsorption was considered a very important step in the photocatalytic process [13]. Therefore, previous adsorption tests were carried out and the results showed that acid pH (3–3.5) is the most indicated for standard dye adsorption on TiO<sub>2</sub> surface. Thus, the degradation of the real textile effluent samples composed mostly of dyes, sodium chloride, and surfactant agents were carried out at pH 3.5. Under this condition, initially reactive dyes (anionic form) were attracted to the semiconductor surface, which was positively charged [14], forming a first layer of dye. The subsequent dye layers were formed following a charge independent adsorption zero-order model, resulting in data that cannot be adjusted to simple adsorption models such as the Langmuir–Hinshelwood one. It should be stressed that it was possible to observe the color appearance and disappearance on the TiO<sub>2</sub> surface in the beginning and final of the degradation process, respectively.

Using a pH close to 3.5 will help to keep the degradation conditions of different advanced oxidation processes as close as possible to each other for comparison sake as this is the purpose of this work. Furthermore, when Fenton reactions are carried out in acid pH the precipitation of Fe(OH)<sub>3</sub> is avoided. Under these conditions, the effluent absorbance decreased significantly for all treatments (Fig. 2); EFC effluent (not shown in the figure) behaved similarly. The absorbance reduction indicates the fragmentation of the organic structures with complete effluent decolorization as well as partial loss of aromatics after irradiation for few minutes. The most effective effluent absorbance reduction in the UV region of the spectrum was obtained to the association of UV/TiO<sub>2</sub>/H<sub>2</sub>O<sub>2</sub> treatment.

These results can be explained by the following reactions: (a) [15] and (b) [16], which present the possible formation of hydroxyl radicals, the main species responsible for the oxidative character of the reaction medium in the studied treatments. The described reactions below indicate that hydroxyl radicals are more likely to form in UV/TiO<sub>2</sub>/H<sub>2</sub>O<sub>2</sub> systems and a larger number of oxidizing species can appear in the e<sup>-</sup>/h<sup>+</sup> generation

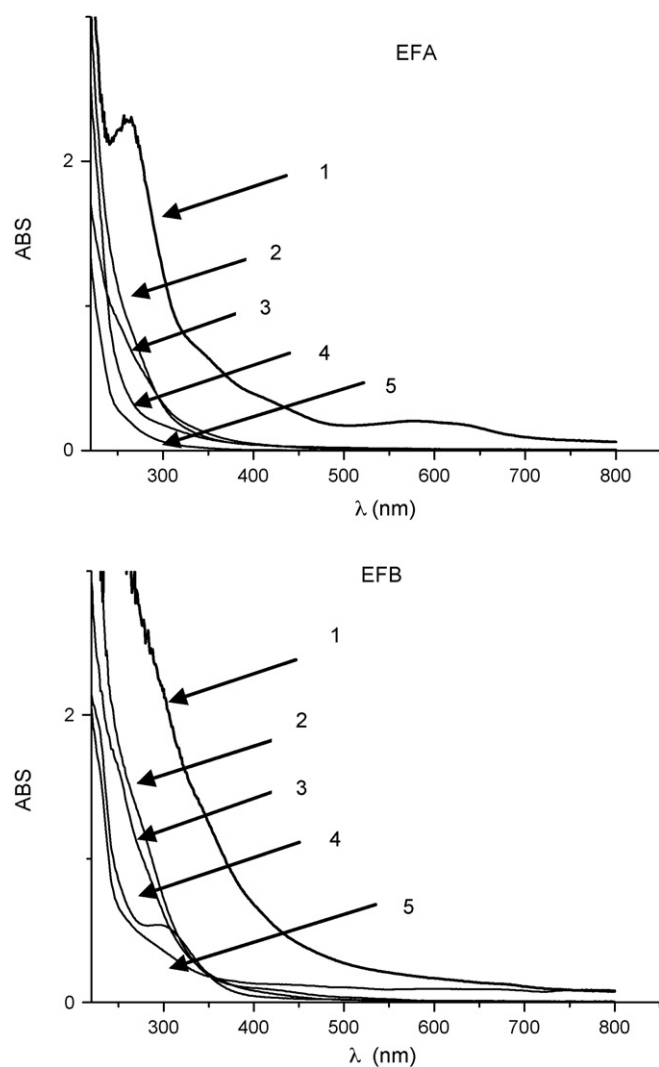
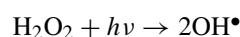


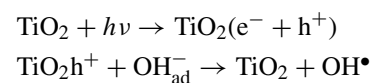
Fig. 2. Reduction in absorbance levels in the EFA and EFB effluents. The different numbers refers to effluent spectra in the following conditions: (1) without treatment; (2) after treatment with H<sub>2</sub>O<sub>2</sub>; (3) after treatment with TiO<sub>2</sub>; (4) after treatment with Fenton reaction; (5) after treatment with TiO<sub>2</sub> plus H<sub>2</sub>O<sub>2</sub>.

process [17].

UV/H<sub>2</sub>O<sub>2</sub> (a)



UV/TiO<sub>2</sub> (a)



UV/H<sub>2</sub>O<sub>2</sub>/TiO<sub>2</sub> (a)

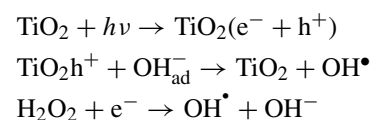
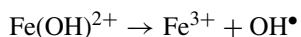


Table 2  
Final concentration of the mineralized products in the real EFA, EFB, and EFC textile effluents for H<sub>2</sub>O<sub>2</sub>, TiO<sub>2</sub>, H<sub>2</sub>O<sub>2</sub>/TiO<sub>2</sub>, Fe<sup>2+</sup>/H<sub>2</sub>O<sub>2</sub> treatments<sup>a</sup>

Sample	Reagents	NH <sub>4</sub> <sup>+</sup> (mg L <sup>-1</sup> )	NO <sub>3</sub> <sup>-</sup> (mg L <sup>-1</sup> )	SO <sub>4</sub> <sup>2-</sup> (mg L <sup>-1</sup> )	COD (mgO <sub>2</sub> L <sup>-1</sup> )	H <sub>2</sub> O <sub>2</sub> (mg L <sup>-1</sup> )
EFA	H <sub>2</sub> O <sub>2</sub>	2.80	0.147	131.68	268.16	n.d.
	TiO <sub>2</sub>	2.94	0.157	134.13	135.60	n.d.
	H <sub>2</sub> O <sub>2</sub> /TiO <sub>2</sub>	3.00	1.580	135.85	72.32	n.d.
	Fe <sup>2+</sup> /H <sub>2</sub> O <sub>2</sub>	6.45	0.668	130.56	334.48	136.41
EFB	H <sub>2</sub> O <sub>2</sub>	1.70	0.199	22.43	226.00	22.71
	TiO <sub>2</sub>	1.75	0.255	61.03	108.98	n.d.
	H <sub>2</sub> O <sub>2</sub> /TiO <sub>2</sub>	6.44	0.433	87.32	99.49	n.d.
	Fe <sup>2+</sup> /H <sub>2</sub> O <sub>2</sub>	3.08	1.343	163.04	298.30	90.54
EFC	H <sub>2</sub> O <sub>2</sub>	11.20	0.318	25.74	289.28	n.d.
	TiO <sub>2</sub>	11.25	n.d.	40.63	126.56	n.d.
	H <sub>2</sub> O <sub>2</sub> /TiO <sub>2</sub>	14.00	1.41	56.07	n.d.	n.d.
	Fe <sup>2+</sup> /H <sub>2</sub> O <sub>2</sub>	2.70	0.202	75.06	131.08	80.94

<sup>a</sup> Organic nitrogen was not detected; n.d.: not detected.

#### UV/Fe<sup>2+</sup>/H<sub>2</sub>O<sub>2</sub> (b)



Nitrogen (azo and amino groups) and sulfur (sulfonic groups) are the main heteroatoms present in reactive dyes, and the characterization of the effluents after the photochemical treatments (Table 2) indicated the formation of inorganic species derived from these heteroatoms. It should be emphasized that the manufacturer that generated the effluents assured us that any inorganic compounds contained either N or S added to the dye solution. Therefore, the only possible source of these species in the solution would be the oxidation of organic compounds. The organic form of nitrogen was not detected in any of the effluents after the oxidation treatments, which indicated the mineralization of the organic effluent species and the possible formation of NH<sub>4</sub><sup>+</sup>, NO<sub>3</sub><sup>-</sup>, and N<sub>2</sub> in the system. Another possibility is the formation of sulfate ions, which confirms the theory. However, the associations of UV/TiO<sub>2</sub>/H<sub>2</sub>O<sub>2</sub> and UV/Fe<sup>2+</sup>/H<sub>2</sub>O<sub>2</sub> proved to be more effective and exhibited the highest mineralization rates for the three tested effluents, followed by the UV/TiO<sub>2</sub> and UV/H<sub>2</sub>O<sub>2</sub> systems, respectively.

As for the species derived from nitrogen, only the formation of NO<sub>3</sub><sup>-</sup> and NH<sub>4</sub><sup>+</sup> ions could be expected, since these are very common products of photocatalytic processes. However, taking into account the complete disappearance of organic nitrogen (Diagram 1), which was the only source of nitrogen before irradiation (1), the formation of stoichiometric amounts was sought for a coherent mass balance. However, total nitrogen balance was not possible for any of the experiments, since the sample matrices were complex and difficult to characterize. In addition, it should be considered that part of the nitrogen can be released

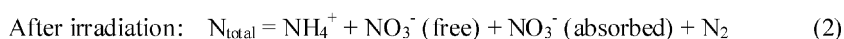
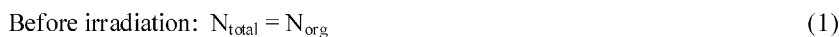


Diagram 1. Nitrogen species in the reaction medium before and after irradiation.

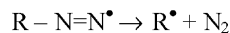
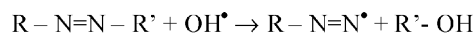


Diagram 2. Formation of N<sub>2</sub> in oxidative processes involving hydroxyl radicals.

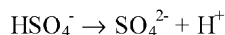
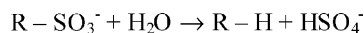


Diagram 3. Formation of sulfate ions during oxidation of dyes.

into the atmosphere and part of NO<sub>3</sub><sup>-</sup> could be absorbed on TiO<sub>2</sub> surface (2).

The N<sub>2</sub> formation process is possible through the following reactions: (a) the azo group of the dyes (–N=N–) could be a possible precursor of N<sub>2</sub>; (b) the azo group atoms are already in zero oxidation state, that is, N<sub>2</sub>. The formation of N<sub>2</sub> from (–N=N–) can be described by a simple radical reaction, as shown in Diagram 2 [18].

The formation of inorganic products concomitantly to COD disappearance also leads to the production of sulfate ions, which is derived from organic sulfur. The advantage of studying the sulfate ion is that the sulfur contained in the dyes is already in its highest oxidation state (6+), thus, the only product expected from this heteroatom is the sulfate ion (Diagram 3) derived from the initial attack to the dye sulfonic groups [18]. The formation of sulfate ions after the oxidation of the EFA effluent sample by using the UV/TiO<sub>2</sub>/H<sub>2</sub>O<sub>2</sub> system (Fig. 3) indicates that SO<sub>4</sub><sup>2-</sup> is formed at a high rate at the beginning of the reaction and then becomes stable. This confirms the theory that the dye sulfonic groups of are attacked in the first minutes of irradiation.

On the other hand, it should be noticed that part of the anions formed in the process may still be adsorbed onto the surface of TiO<sub>2</sub> in the case of the heterogeneous photocatalysis. As previously discussed, at acidic pH, the surface is positively charged

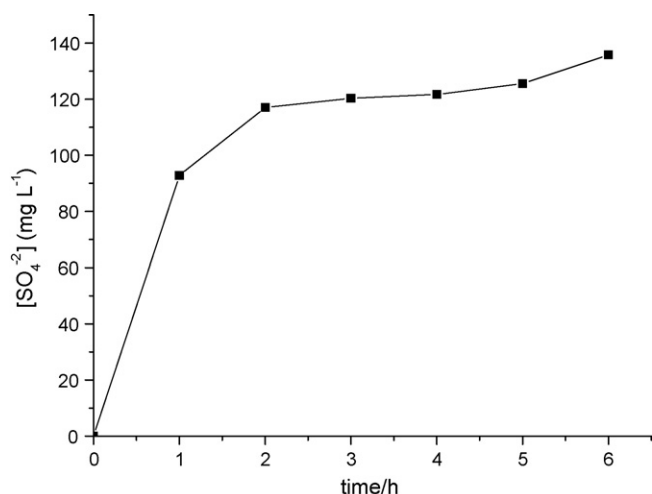


Fig. 3. Evolution of the sulfate ions in the EFA effluent during UV/TiO<sub>2</sub>/H<sub>2</sub>O<sub>2</sub> treatment.

and control experiments indicated an adsorption of approximately 10% of the sulfate and nitrate ions under the same irradiation conditions and in standard condition.

Data concerning COD reduction also indicate that the most effective mineralization process was UV/TiO<sub>2</sub>/H<sub>2</sub>O<sub>2</sub>, because it reached reduction levels higher than 90%, whereas the use of only peroxide or Fenton reagent resulted in COD reductions of 60% and 80%, respectively. The treatment associating UV/TiO<sub>2</sub>/H<sub>2</sub>O<sub>2</sub> consumed the added peroxide completely, whereas the Fenton reactions yet presented H<sub>2</sub>O<sub>2</sub> at the end. Furthermore, the UV/TiO<sub>2</sub>/H<sub>2</sub>O<sub>2</sub> treatment has the advantage of leads to a final nontoxic residue due to the absence of residual peroxide. The final peroxide concentrations associated with the Fenton reactions were around 38%, 25%, and 23% for effluents EFA, EFB, and EFC, respectively.

Since the most effective treatment was the association of UV/TiO<sub>2</sub>/H<sub>2</sub>O<sub>2</sub>, the degradation kinetic behaviors were analyzed for this condition. The results indicate that the degradation of the effluents happens through pseudo-first-order reactions, as

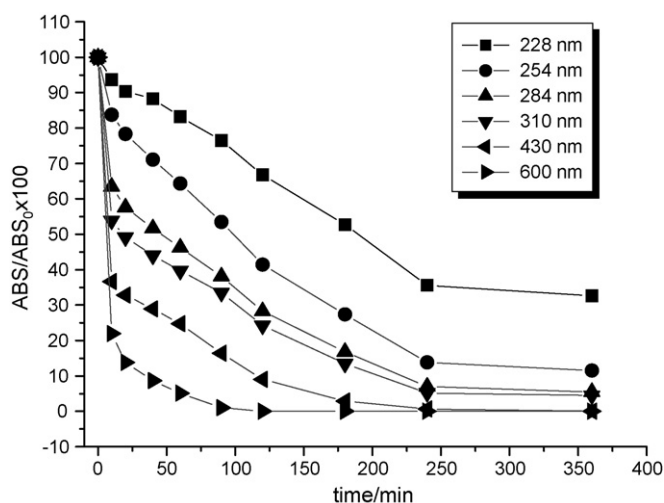


Fig. 4. Monitoring of absorbance decay during 6 h of EFB effluent irradiation under UV/TiO<sub>2</sub>/H<sub>2</sub>O<sub>2</sub> treatment.

well as in most of the degradation experiments. The plots of  $\ln C/C_0$  versus time for this kind of experiments are straight lines and provide the angular coefficients, which correspond to the numerical values for the degradation rate constants ( $k$ ). Assuming that the concentration of hydroxyl radicals is higher than that of substrate leads to Eq. (1):

$$\ln \left( \frac{C_t}{C_0} \right) = -kt \quad (1)$$

where  $C_0$  is the initial concentration,  $C_t$  the concentration of substrate at a given time,  $t$  the time, and  $k$  is the velocity constant ( $t^{-1}$ ) [19]. Fig. 4 shows the absorbance decay in different wavelengths as a function of irradiation time to the EFB effluent sample during irradiation process. It can be noticed that decolorization happens very fast (in the first minutes of irradiation), whereas the loss of simple and conjugated aromatics compounds is slower and more gradual. This happens because degradation begins with the rupture of structures more suscepti-

Table 3

Degradation percentages (in terms of absorbance reduction<sup>a</sup>) and rate constants ( $k$ ) for EFA, EFB, and EFC effluents in relevant wavelengths (H: H<sub>2</sub>O<sub>2</sub>; T: TiO<sub>2</sub>; TH: TiO<sub>2</sub>/H<sub>2</sub>O<sub>2</sub>; F: Fenton)

Sample	254 nm	284 nm	310 nm	430 nm
<b>EFA (H)</b>				
Degradation %	52.91	70.33	76.88	90.67
$k$ (min <sup>-1</sup> )	0.0016	0.0019	0.0022	0.0033
$R$	0.991	0.973	0.990	0.992
<b>EFA (T)</b>				
Degradation %	61.66	72.44	74.33	90.35
$k$ (min <sup>-1</sup> )	0.0018	0.0021	0.0030	0.0035
$R$	0.998	0.998	0.996	0.993
<b>EFA (TH)</b>				
Degradation %	87.97	94.58	95.51	100
$k$ (min <sup>-1</sup> )	0.0059	0.0075	0.0078	0.017
$R$	0.994	0.988	0.995	0.984
<b>EFA (F)</b>				
Degradation %	27.59	32.07	34.63	57.14
$k$ (min <sup>-1</sup> )	<sub>b</sub>	<sub>b</sub>	<sub>b</sub>	<sub>b</sub>
$R$	<sub>b</sub>	<sub>b</sub>	<sub>b</sub>	<sub>b</sub>
<b>EFB (H)</b>				
Degradation %	36.99	56.35	59.62	78.42
$k$ (min <sup>-1</sup> )	0.0015	8.92.10 <sup>-4</sup>	0.0014	0.0024
$R$	0.975	0.981	0.963	0.974
<b>EFB(T)</b>				
Degradation %	49.16	56.21	65.94	86.05
$k$ (min <sup>-1</sup> )	0.0016	<sub>b</sub>	<sub>b</sub>	0.0053
$R$	0.941	<sub>b</sub>	<sub>b</sub>	0.970
<b>EFB (TH)</b>				
Degradation %	74.92	82.36	87.29	67.36
$k$ (min <sup>-1</sup> )	0.012	0.014	0.015	0.011
$R$	0.996	0.976	0.978	0.982
<b>EFB (F)</b>				
Degradation %	34.69	46.29	48.09	68.53
$k$ (min <sup>-1</sup> )	<sub>b</sub>	<sub>b</sub>	<sub>b</sub>	<sub>b</sub>
$R$	<sub>b</sub>	<sub>b</sub>	<sub>b</sub>	<sub>b</sub>

<sup>a</sup> (Absorbance after treatment/absorbance before treatment initial) × 100.

<sup>b</sup> It did not exhibit a linear behavior during degradation.

ble to oxidation, such as the azo groups, which originate smaller compounds that undergo further oxidation until attain a complete mineralization.

The efficiency of different treatments in the degradation of EFA and EFB effluents can be compared in terms of degradation percentage, rate constants, and the linear regression coefficients (Table 3). The Fenton reactions gave the smallest absorbance reduction level at 254 nm. This is caused by the presence of residual hydrogen peroxide in the solution since control tests point to interference in spectral absorbance at this wavelength at high concentrations of peroxide.

#### 4. Conclusion

The obtained results prove that the treatment of textile effluents using advanced oxidation processes with UV radiation is effective for decolorization, COD reduction, and mineralization in short irradiation time. The fact that these treatment processes do not generate residues justifies the use of any of the techniques. The general efficiency presented by the techniques decreased as following:  $UV/TiO_2/H_2O_2 > UV/Fe^{2+}/H_2O_2 > UV/TiO_2 > UV/H_2O_2$ . More detailed studies would be necessary in order to optimize these techniques for industrial scale. Nevertheless, studies such as this one already indicate that it is possible to implement this kind of waste treatment, particularly in the textile industry, since the matrices of this kind of effluents are not easily biodegradable.

#### Acknowledgement

CNPq, Capes, Fundação Araucária, MR Malharia.

#### References

- [1] R.L. Cisneros, A.G. Espinoza, M.I. Litter, Photodegradation of an azo dye of the textile industry, *Chemosphere* 48 (2002) 393–399.
- [2] C.C.I. Guaratini, M.V.B. Zanoni, Corantes Têxteis, *Química Nova* 23 (2000) 71–77.
- [3] Y.E. Benkli, M.F. Can, M. Turan, M.S. Çelik, Modification of organo-zeolite surface for the removal of reactive azo dyes in fixed-bed reactors, *Water Res.* 39 (2005) 487–493.
- [4] H. Selcuk, Decolorization and detoxification of textile wastewater by ozonation and coagulation processes, *Dyes Pigments* 64 (2005) 217–222.
- [5] S.M. Ghoreishi, R. Haghghi, Chemical catalytic reaction and biological oxidation for treatment of non-biodegradable textile effluent, *Chem. Eng. J.* 95 (2003) 163–169.
- [6] M.A. Hauf, S. Ashraf, S.N. Alhadrami, Photolytic oxidation of Coomassie Brilliant Blue with  $H_2O_2$ , *Dyes Pigments* 66 (2005) 197–2000.
- [7] M.H. Habibi, A. Hassanzadeh, S. Mahdavi, The effect of operational parameters on the photocatalytic degradation of three textile azo dyes in aqueous  $TiO_2$  suspensions, *J. Photochem. Photobiol. A: Chem.* 172 (2005) 89–96.
- [8] D. Yu, R. Cai, Z. Liu, Studies on the photodegradation of Rhodamine dyes on nanometer-sized zinc oxide, *Spectrochim. Acta A: Mol. Biomol. Spectrosc.* 60 (2004) 1617–1624.
- [9] J.M. Chacón, M.T. Leal, M. Sánchez, E.R. Bandala, Solar photocatalytic degradation of azo-dyes by photo-Fenton process, *Dyes Pigments* 69 (2005) 144–150.
- [10] A.O. Martins, V.M. Canalli, C.M.N. Azevedo, M. Pires, Degradation of pararosaniline (C.I. Basic Red 9 monohydrochloride) dye by ozonation and sonolysis, *Dyes Pigments* 68 (2005) 227–234.
- [11] APHA—American Public Health Association, Standard Methods for the Examination of Water and Wastewater, AWWA, WPCF, Washington, DC, 1998.
- [12] M.R.A. Silva, M.C. Oliveira, R.F.P. Nogueira, Estudo da aplicação do processo Foto-Fenton solar na degradação de efluentes de indústrias de tintas, *Eclética Química* 29 (2004) 19–26.
- [13] Y. Chen, S. Yang, K. Wang, L. Lou, Role of primary active species and  $TiO_2$  surface characteristics in UV-illuminated photodegradation of Acid Orange 7, *J. Photochem. Photobiol. A: Chem.* 172 (2005) 47–54.
- [14] Y. Wang, C.S. Hong, F. Fang, Effect of solution matrix on  $TiO_2$  photocatalytic degradation of 2-chlorobiphenil, *Environ. Eng. Sci.* 16 (1999) 433–440.
- [15] S. Malato, J. Blanco, A. Vidal, D. Alarcón, M.I. Maldonado, J. Cáceres, W. Gernjak, Applied studies in solar photocatalytic detoxification: an overview, *Sol. Energy* 75 (2003) 329–336.
- [16] Y. Xie, F. Chen, J. He, J. Zhao, H. Wang, Photoassisted degradation of dyes in the presence of  $Fe^{3+}$  and  $H_2O_2$  under visible radiation, *J. Photochem. Photobiol. A: Chem.* 136 (2000) 235–240.
- [17] M.R. Hoffmann, S.T. Martin, W. Choi, D.W. Bahnemann, Environmental applications of semiconductor photocatalysis, *Chem. Rev.* 95 (1995) 69–96.
- [18] M. Karkmaz, E. Puzenat, C. Guillard, J.M. Herrmann, Photocatalytic degradation of the alimentary azo dye amaranth. Mineralization of the azo group to nitrogen, *Appl. Catal. B: Environ.* 51 (2004) 183–194.
- [19] C. Lizama, J. Freer, J. Baeza, H. Mansilla, Optimized photodegradation of reactive blue 19 on  $TiO_2$  and ZnO suspension, *Catal. Today* 76 (2002) 235–246.